

Dynamics of the nuclear spin polarization by optically oriented electrons in a (In,Ga)As/GaAs quantum dot ensemble

Roman V. Cherbunin,^{1,2} Sergey Yu. Verbin,^{1,2} Thomas Auer,¹ Dmitri R. Yakovlev,^{1,3} Dirk Reuter,⁴ Andreas D. Wieck,⁴ Ilya Ya. Gerlovin,² Ivan V. Ignatiev,^{1,2} Dmitry V. Vishnevsky,² and Manfred Bayer¹

¹*Experimentelle Physik II, Technische Universität Dortmund, 44221 Dortmund, Germany*

²*Faculty of Physics, St. Petersburg State University, 198504 St. Petersburg, Russia*

³*Ioffe Physico-Technical Institute, Russian Academy of Sciences, 194021 St. Petersburg, Russia*

⁴*Angewandte Festkörperphysik, Ruhr-Universität Bochum, 44780 Bochum, Germany*

(Received 27 December 2008; revised manuscript received 9 April 2009; published 28 July 2009)

The nuclear spin dynamics in an ensemble of singly charged (In,Ga)As/GaAs quantum dots has been studied at a temperature of 1.6 K. The effective magnetic field of nuclear polarization was detected through the circular polarization of quantum dot photoluminescence. The polarization is reduced if an external magnetic field compensates the nuclear field. To study the time evolution of the nuclear field, a photoluminescence pump-probe technique has been developed, from which we find a complex behavior of the nuclear-polarization dynamics; its rise is considerably slowed down when the effective field of polarized nuclei exceeds that of the nuclear spin fluctuations. A phenomenological model for the dynamics of a strongly coupled electron-nuclear spin system has been developed, whose results qualitatively agree with the experimental data.

DOI: [10.1103/PhysRevB.80.035326](https://doi.org/10.1103/PhysRevB.80.035326)

PACS number(s): 78.67.Hc, 72.25.Fe, 71.70.Jp

I. INTRODUCTION

The nuclear and electron-spin systems in semiconductor quantum dots (QDs) constitutes a coupled quantum-mechanical system due to the strong hyperfine interaction between them.¹⁻³ Due to various proposals of spin-based devices, research on the electron-nuclear spin dynamics in QDs is subject of great current interest, both experimentally⁴⁻⁸ and theoretically.⁹⁻¹⁴ In absence of an external magnetic field, the interaction with randomly oriented nuclear spins is usually considered as the most efficient mechanism of electron-spin-polarization decay in QDs.^{9,15} Optical orientation of nuclear spins by interaction with a polarized electron spin may suppress this process and, therefore, increase the electron-spin polarization lifetime.⁴

The experimental method for studying nuclear spin polarization in QDs has up to now been utilizing the change in Zeeman splitting of exciton emission lines due to hyperfine interaction with polarized nuclear spins (Overhauser shift). Thereby the nuclear polarization under steady-state excitation conditions^{3,5,8} as well as its dynamics⁶ could be addressed. Because of the large inhomogeneities in a QD ensemble, such measurements have to be performed on a single QD.^{3,5,6,8}

There has been no effective method for studying the dynamics of nuclear spin polarization in a QD *ensemble* so far. In our work, we demonstrate such a method to determine the effective magnetic field of the dynamic nuclear polarization (DNP) and apply it successfully to an (In,Ga)As/GaAs QD ensemble for moderate optical excitation densities. Due to the sensitivity of the applied method, we determine the nuclear spin polarization as well as its variation in the ensemble and find that the variation in the optically created nuclear field is about its average value. Time-resolved studies reveal a nontrivial dependence of the nuclear spin dynamics on optical excitation density, in agreement with theoretical predictions.^{13,14}

The information derived in that way is complementary to the one obtained by single-dot studies, which represent a single snapshot taken from an ensemble with its unavoidable inhomogeneities. Due to these inhomogeneities, information about the statistical variation is needed. Developing these statistics from single-dot studies is cumbersome because of the complexity of the experiment so that ensemble studies are appealing. From first sight this is counterintuitive because of the rather small relevant energy scales as compared to the sizeable variations. The fact that we obtain unique values from ensemble demonstrates, however, the validity of the approach.

II. EXPERIMENT

We studied a heterostructure containing 20 layers of self-assembled (In,Ga)As QDs sandwiched between GaAs barriers with n -delta modulation-doped sheets.¹⁶ Donor ionization supplies every dot with on average a single resident electron. The structure was grown by molecular beam epitaxy on a (100) GaAs substrate. Rapid thermal postgrowth annealing shifted the lowest QD optical transition to energies around 1.34 eV. The sample was mounted in a cryostat with a superconducting magnet for fields, B , parallel to the optical excitation and detection axis (Faraday geometry). The experiments were performed with the sample immersed in pumped liquid helium at a temperature of $T=1.6$ K. Photoluminescence (PL) was excited by a continuous-wave Ti:Sapphire laser, dispersed by a 0.5 m spectrometer and detected with a silicon avalanche photodiode. The PL polarization was measured using a photoelastic modulator operated at a frequency of 50 kHz and a multichannel photon-counting system. The time resolution for detection of the PL polarization was limited to 20 μ s. Special timing protocols for optical excitation and PL detection were developed to study the dynamics of nuclear polarization, as described in detail in Sec. IV.

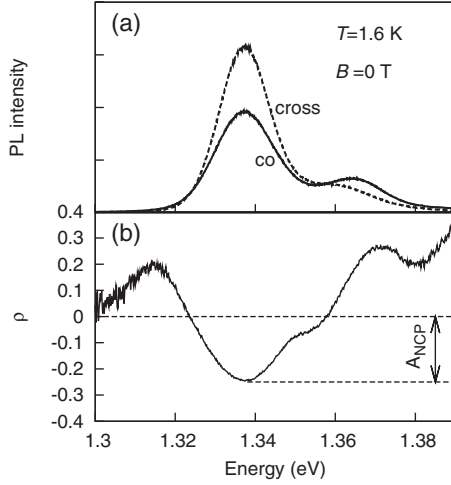


FIG. 1. (a) PL spectra of (In,Ga)As/GaAs QDs for σ^+ -polarized excitation measured in copolarization (σ^+ , solid line) and cross (σ^- , dashed line) polarization. Excitation energy is 1.459 eV; power density $I_{exc}=3$ W/cm²; and $T=1.6$ K. (b) Degree of PL circular polarization calculated by: $\rho=(I^{++}-I^{--})/(I^{++}+I^{--})$, where I^{++} (I^{--}) is PL intensity for copolarization (crosspolarization) of excitation and detection. The polarization is negative for emission from QD ground state at 1.34 eV and positive for excited state emission at 1.37 eV.

The DNP was determined from the circular-polarization degree of the QD-ensemble photoluminescence excited at the low-energy wing of the wetting-layer optical transition. The PL polarization of singly negatively charged QDs is negative, i.e., the PL is predominantly σ^- polarized for σ^+ -polarized optical excitation as shown in Fig. 1. The mechanism of negative circular polarization (NCP) has been extensively discussed in literature^{17–22} and is attributed to optical orientation of the resident electron spins. The amplitude of the NCP [see definition of A_{NCP} in Fig. 1(b)] is proportional to the mean electron-spin polarization along the optical axis, S_z , in the QD ensemble²²

$$A_{NCP} \approx 2S_z. \quad (1)$$

The NCP is solely used here to monitor electron and nuclei spin polarization created by off-resonant optical excitation. The magnetic-field dependence of the electron spin polarization reveals a dip at weak magnetic fields, which is related to depolarization of the electron spins by the effective magnetic field of the nuclear spin fluctuations.^{15,23} According to Ref. 15, the polarization degree at the dip center can be as small as one third of full polarization if the fluctuations are “frozen” and decreases further to smaller value if the fluctuations become “melted.” In the absence of DNP, the dip is centered at zero external magnetic field. Polarization of the nuclei via hyperfine interaction with the optically oriented electrons may result in appearance of an effective magnetic field (hereafter referred to as the nuclear or DNP field, B_N) acting on the electron spin together with the external magnetic field. This nuclear field is expected to shift the polarization dip from zero external field where the shift direction is determined by the circular-polarization helicity of the optical

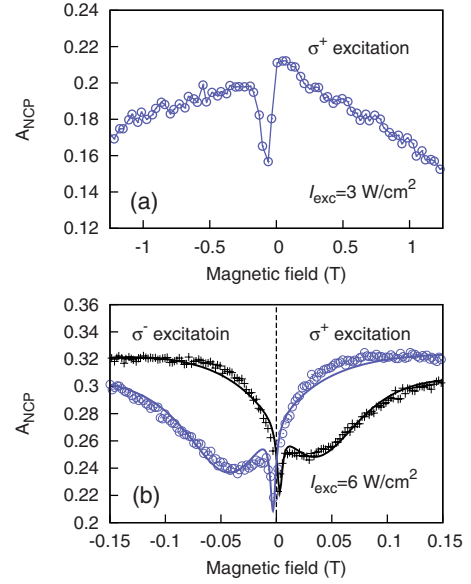


FIG. 2. (Color online) (a) Dependence of absolute value of circular-polarization degree of PL, $|\rho|$, measured for a fixed polarization of weak optical excitation in a large range of longitudinal magnetic fields. $T=1.6$ K. (b) Polarization dependencies measured for σ^+ and σ^- excitation in a narrow range around zero magnetic field (symbols). Lines are fits using Eq. (2) with a magnetic-field-dependent nuclear field (see text).

pumping. By measuring the shift, one can estimate the strength of the DNP field.

III. DNP FOR FIXED POLARIZATION OF OPTICAL EXCITATION

Experimentally measured magnetic-field dependencies of the PL polarization are shown in Fig. 2. Panel (a) shows the dependence measured over a large range of magnetic fields. The overall dependence has a bell-like shape related to suppression of the NCP mechanism by strong magnetic fields.^{18–20} We focus here on the narrow range around zero magnetic field, shown in panel (b) for opposite optical-excitation polarizations. The magnetic-field dependence consists of a narrow dip positioned close to zero magnetic field and of a wider dip shifted from zero field.

The narrow dip is commonly ascribed to the compensation of the electron Knight field by the external magnetic field.²⁴ Under compensation, the nuclear spins rapidly relax by dipole-dipole interaction. Contact interaction of the electron with the relaxing nuclei results in the observed decrease in the electron-spin polarization.

The wider dip shifted from zero field by about 40 mT results from depolarization of the electron spin by frozen nuclear spin fluctuations. The shift direction depends on the excitation helicity. Therefore we attribute the shift to the appearance of a nuclear field created by optical pumping. The conclusion that the shift of the wide dip is related to the DNP field is further supported by data obtained for different excitation densities. The corresponding data are shown in Fig. 3(a). The magnetic-field dependence of the PL polarization at

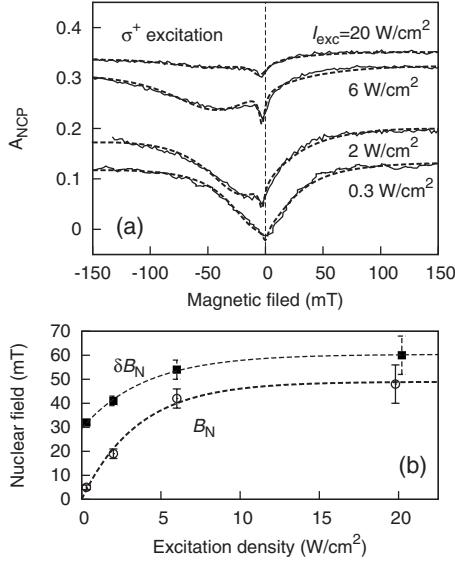


FIG. 3. (a) Magnetic-field dependence of PL polarization measured for fixed excitation polarization at different power densities (Ref. 25). Dashed lines are fits by a function which combines Eq. (2) with an additional term modeling the Knight dip (see text). (b) Dependencies of nuclear field and of its spread on excitation density obtained from the fits shown in panel (a). Lines are guides to the eye.

low excitation ($I_{exc} \leq 0.3 \text{ W/cm}^2$) shows the expected dip centered at $B=0$. With increasing power density the wide dip is continuously shifted to higher B , evidencing an increasing effective nuclear magnetic field due to DNP. Figure 3(a) also shows an overall increase in the PL polarization with excitation density, which is related to a change in the balance between optical orientation and relaxation of the electron spin. We will not discuss this effect in detail here.

To estimate the created DNP field quantitatively, we recently developed an approximative description of the experimental dependencies. The polarization dip in absence of a nuclear field ($B_N=0$) can be well described by a Lorentz profile.²³ We will use this approximation also for the case of a nonzero nuclear field B_N with half-width at half maximum (HWHM) δB_N to fit the main part of the polarization dip

$$\rho(B) = \rho(\infty) \left(1 - \frac{A_{dip}}{1 + [(B + B_N)/\delta B_N]^2} \right). \quad (2)$$

Here $\rho(\infty)$ is the PL-polarization degree at large magnetic fields and A_{dip} is the dip depth. Note that B_N is considered here as the average nuclear field in the QD ensemble. The validity of this approach will be discussed in Sec. V.

To approximate the experimental dependencies, we also take into account the mentioned destruction of the electron-spin polarization when the external field compensates the Knight field.²⁰ We model the narrow dip caused by this destruction by a function similar to Eq. (2), replacing the parameters B_N and δB_N with B_e and δB_e , which describe the average Knight field and its variation in the ensemble, respectively. Both parameters amount to about 2 mT, depending weakly on the experimental conditions. Fits obtained in

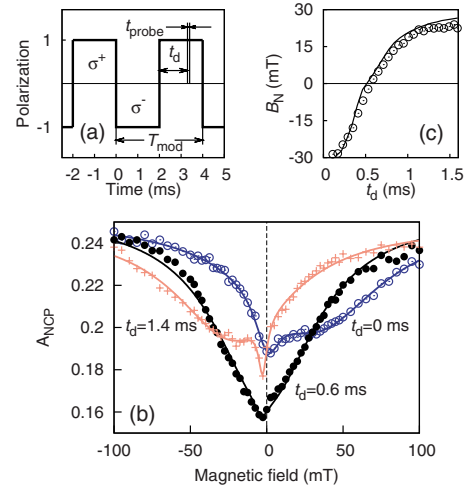


FIG. 4. (Color online) (a) Timing protocol for the polarization modulation of optical excitation. Levels 1 and -1 correspond to σ^+ and σ^- polarizations, respectively. (b) Magnetic-field dependence of PL-polarization degree measured at different times, t_d , within the second half period after changing the excitation polarization (symbols). Modulation period $T_{mod}=4$ ms; detection window $t_{probe}=0.1$ ms, and excitation density $I_{exc}=5 \text{ W/cm}^2$. Lines are fits to the data as described in text. (c) Time dependence of dip position obtained from fits of the experimental data (circles) and from our model (line, see Sec. V) with parameters: $P=150 \text{ T/s}$, $\tau_{dd}=0.1$ ms, $\tau_{N1}=1$ ms, $B_{f\rho}=18$ mT, $B_I=1$ mT, and $B_e=2$ mT.

that way are shown in Figs. 2(b) and 3(a) by lines. They allow us to extract B_N and δB_N with high accuracy.

Figure 3(b) shows the dependencies of B_N and δB_N on optical excitation density. As expected, the dip shift and, correspondingly, the average nuclear field increase with excitation density. However, this increase saturates at a level of several tens of milliTesla at the largest pumping of 20 W/cm^2 used here. The dip shift is accompanied by an approximately twofold increase in its width, which reflects an increase in the nuclear-field spread. Simultaneously, the dip depth is considerably reduced so that the dip becomes hardly visible at large excitation density. The depth reduction is stronger than the dip broadening so that the dip area decreases. This effect limits the applicability of our method for studying DNP to relatively low excitation densities only.

The origin of so fast decrease in the dip depth is not entirely clear so far. The modeling of the nuclear spin dynamics described in Sec. V shows that the decrease is partially due to the spread of nuclear spin pumping rates. In addition, the spread of the QD parameters in the ensemble probably gives rise to further broadening of the dip and decrease in its depth.

IV. KINETICS EXPERIMENTS

For studying the dynamics of the nuclear polarization the sample was excited by circularly polarized light whose helicity was periodically changed, as shown in Fig. 4(a). For that purpose the excitation polarization was modulated by an electro-optical modulator (EOM) followed by a quarter-wave plate. A alternating sequence of σ^+ - and σ^- -polarized pulses

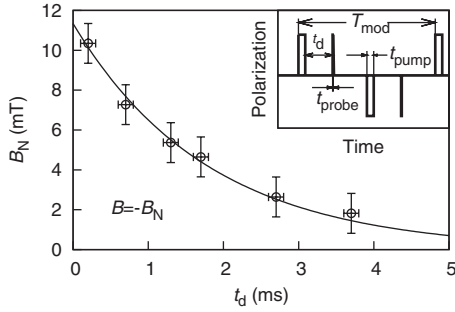


FIG. 5. Dependence of dip position on dark time, t_{dark} , between pump and probe pulses. Experimental data are shown by symbols. $I_{exc}=1 \text{ W/cm}^2$. Line is exponential fit by $y=c \exp(-t/\tau_N)$, with $\tau_N=1.8 \text{ ms}$. Inset shows timing protocol of excitation and polarization modulation. The pump and probe pulses have the same peak intensity but different durations: $t_{pump}=1 \text{ ms}$ and $t_{probe}=0.2 \text{ ms}$. Modulation period $T_{mod}=20 \text{ ms}$.

with sharp rising and falling edges of about 100 ns was created in that way. The illumination time for each helicity, t_{pump} , was equal to half of the modulation period T_{mod} . The PL-polarization degree was measured in a time window, t_{probe} . This time window was shifted by a delay time t_d from the polarization switching moment through the modulation half period. The timing protocol is shown in Fig. 4(a).

Examples of experimental dependencies of the PL polarization on magnetic field are shown in Fig. 4(b). The shift of the detection time window is accompanied by a continuous shift of the polarization dip along the magnetic field axis, reflecting the change in the DNP field with time.

The DNP-field evolution obtained by fitting the magnetic-field dependencies is shown in Fig. 4(c). The field varies from -30 mT attained at the end of the previous half period of modulation with σ^- excitation to approximately same but positive value of $+30 \text{ mT}$ at the end of the modulation period. The variation is rather slow at the beginning, then becomes faster, and finally is slowed down again toward the end of this half period. When the excitation polarization is switched again, the DNP field changes in a similar way in reverse direction (not shown here).

The deceleration of the DNP field rise near the end of the half period may be caused by slowing of the nuclear spin pumping rate, as proposed theoretically,^{13,14} or by relaxation of the nuclear spin polarization. The latter plays significant role if the relaxation time is shorter than the period of modulation.

To estimate the relaxation time, we studied the nuclear spin dynamics without illumination, i.e., in a dark interval after blocking the optical pumping. The used timing protocol is shown in the inset of Fig. 5. The electron-spin polarization was measured during a relatively short probe pulse ($t_{probe}=0.2 \text{ ms}$) delayed relative to the 1 ms pump pulse by a dark-time interval, t_{dark} , whose value was varied from zero up to several ms. The pump- and probe-pulse sequence was shaped by an acousto-optical modulator (AOM) placed in front of an EOM. The polarization of each pulse could be controlled independently by the EOM. We used a series of four pulses of opposite polarizations (two pump and two probe pulses) within a modulation period to obtain zero net nuclear polarization under optical excitation.

Results of measurements of the DNP field as function of t_{dark} are shown in Fig. 5 for the relatively low excitation density of 1 W/cm^2 . The nuclear field decays with a characteristic time $\tau_N=1.8 \text{ ms}$, which is comparable with the period of modulation. Therefore the relaxation process affects considerably the nuclear spin dynamics in the experiments described above. This surprisingly short relaxation time compared to values reported in literature^{1,3,26} will be discussed in Sec. VI.

V. MODEL OF NUCLEAR SPIN ORIENTATION

The majority of publications on dynamic nuclear polarization via interaction with optically oriented electron spins uses, for the analysis of experimental data, the theory developed by Dyakonov and Perel.²⁷ This theory assumes that the electron-spin correlation time determined by temporal fluctuations of the nuclear field is considerably shorter than the precession period of the electron spin in the average nuclear field (see, e.g., Refs. 1, 6, and 28–30). In this case, the electron and nuclear spins can be considered as two separate spin systems, whose interaction can be treated as perturbation causing mutual flips (flip flops) between the electron and nuclear spins. The DNP under optical excitation is considered then as a sequence of two independent processes, namely, (i) the optical orientation of the electron spin and (ii) the flip-flop process giving rise to angular momentum transfer from the electron to the nuclei. The Zeeman splittings of the electron and nuclear spin states in an external magnetic field drastically differ so that flip flops become possible only if the energy uncertainty of the electron state due to the short electron-spin correlation time τ_{el} is larger than the electron Zeeman splitting.

For an electron localized in a QD, the relation between the two above time scales is reversed: the period of electron-spin precession in nuclear field is shorter than the electron-spin correlation time. The precession is on a nanosecond or even subnanosecond time scale whereas relaxation processes for electron and nuclear spins in QDs occur in the microsecond time range.^{15,19} A simple estimate shows that the correlation time exceeds not only the precession period but also the average time between electron-spin polarization events, which is about 100 ns for an excitation density $I_{exc}=10 \text{ W/cm}^2$. We, therefore, can conclude that there is *the coherent evolution* of strongly coupled electron-nuclear spin system in a QD between the polarization events. Absorption of a photon followed by emission of another photon of opposite helicity (which corresponds to a polarization event) introduces angular momentum into the system. Reiterated polarization events give rise to accumulation of angular momentum in the nuclear spin ensemble, i.e., to DNP. It is important that the optical excitation polarizes the coupled electron-nuclear spin system rather than an isolated electron spin. The energy mismatch between the Zeeman splittings of electron and nuclear spin states is not essential for this process due to the large energy difference in absorbed and emitted photons.³¹

The dynamics of the electron-nuclear spin system can be numerically modeled for a relatively small number of nuclei

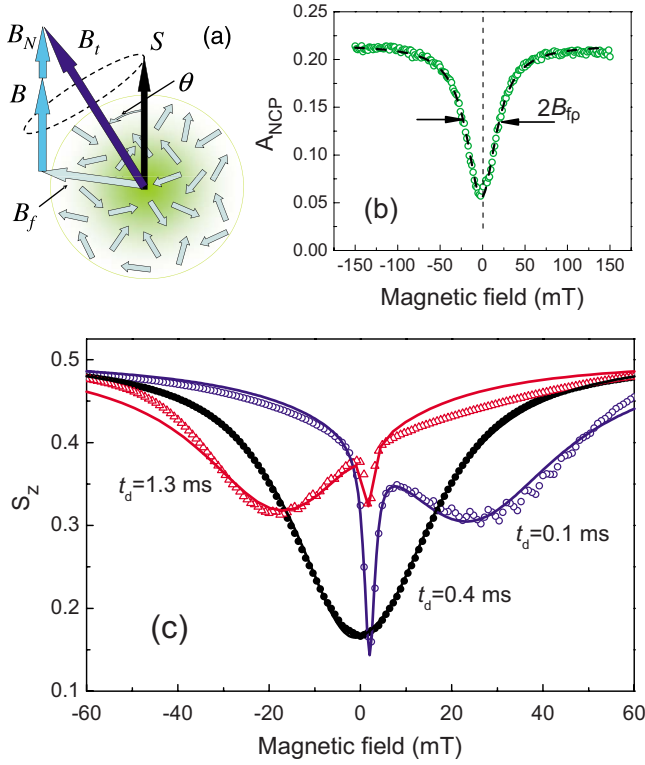


FIG. 6. (Color online) (a) Precession of electron spin about total magnetic field, \mathbf{B}_t , which is the sum of external field, DNP field, and NSF field. (b) Magnetic-field dependence of PL polarization measured for fast modulation of the excitation polarization: $T_{mod} = 10 \mu\text{s}$ and $I_{exc} = 1 \text{ W/cm}^2$. HWHM of the dip is determined by the transverse component of nuclear spin fluctuations, $B_{fp} = 18 \text{ mT}$. (c) Magnetic-field dependence of electron-spin polarization calculated for different times after switching the excitation polarization: $t_d = 0.1 \text{ ms}$ (blue open circles), 0.4 ms (black closed circles), and 1.3 ms (red triangles). Modulation period $T_{mod} = 3.2 \text{ ms}$ and pump rate $P = 150 \text{ T/s}$. Lines are fits by Lorentzians.

only.^{13,14} Therefore we use a phenomenological approach for modeling the experimental data. The model assumes that the nuclear spin system acts on the electron spin as an effective magnetic field. This nuclear field consists of a regular contribution (DNP field), \mathbf{B}_N , created by optical excitation and an irregular one, \mathbf{B}_f , which is the field of the nuclear spin fluctuations (NSF).¹⁵ The latter is related to random correlations among nuclear spins and its magnitude is proportional to B_{Nmax} / \sqrt{N} , where B_{Nmax} is the maximal possible nuclear field for complete nuclear spin polarization of the N nuclei in the QD. This number of nuclei $N \sim 10^5$ in our dots, therefore the fluctuating field should be on the order of a few tens of milliTesla.²³ The total field, \mathbf{B}_t , acting on the electron spin is the sum of external magnetic field, \mathbf{B} , and effective nuclear field, $\mathbf{B}_f + \mathbf{B}_N$, as schematically shown in Fig. 6(a). The field \mathbf{B}_t is tilted from the optical axis by an angle θ given by

$$\sin^2 \theta = \frac{B_{fp}^2}{(B + B_N + B_{fz})^2 + B_{fp}^2}, \quad (3)$$

where B_{fz} and B_{fp} are the longitudinal and transverse components of the NSF field, respectively.

Due to precession of the electron spin about the tilted field, the probability to find the electron in spin state $|+\frac{1}{2}\rangle$ or $|-\frac{1}{2}\rangle$ varies with time even in absence of relaxation processes, according to³²

$$P_{+1/2} = \cos^2(\omega t/2) + \sin^2(\omega t/2)\cos^2 \theta, \\ P_{-1/2} = \sin^2(\omega t/2)\sin^2 \theta, \quad (4)$$

with the precession frequency $\omega = g_e \mu_B B_t / \hbar$. Here g_e is the electron g factor, μ_B is the Bohr magneton, and \hbar is the Planck constant. Here it has been assumed that the electron spin has been initially polarized in the state $|+\frac{1}{2}\rangle$.

Angular momentum can be transferred from a photon to the electron-nuclear spin system if the electron spin is in state $|-\frac{1}{2}\rangle$. Therefore the rate of electron spin polarization averaged over the electron-spin precession is proportional to $\langle P_{-1/2} \rangle = 1/2 \sin^2 \theta$. We want to stress here that this rate is zero if there is no transverse component of the total field. From this consideration the crucial role of the NSF transverse component for the polarization mechanism becomes clear.

Each polarization event is accompanied by transfer of angular momentum from the electron to the nuclear spin system so that the dynamics of DNP can be described by the rate equation

$$\frac{dB_N}{dt} = P \sin^2 \theta - \frac{B_N}{\tau_N}. \quad (5)$$

Here P is proportional to the excitation power density. The second term describes the DNP field relaxation. Because the mechanism of fast nuclear spin relaxation is not fully understood at the moment (see discussion below), we describe this process phenomenologically by an exponential decay which is consistent with our experiment.

To examine the applicability of the proposed model we have solved Eq. (5) numerically with P and τ_N as fitting parameters. The calculations have been done in the following way. First, the time dependence of the nuclear field, $B_N = f_B(t)$, is determined from Eq. (5) keeping the external magnetic field B fixed. Then, using solutions for different B , the dependence of the nuclear field on external magnetic field, $B_N = f_t(B)$, is determined for a fixed time t . In these calculations, we take into account an acceleration of the nuclear spin relaxation due to the dipole-dipole interaction of the nuclear spins when the external magnetic field B compensates the Knight field B_e . The contribution of this process to the relaxation rate has the form¹

$$\frac{1}{\tau_{N0}} = \frac{1}{\tau_{dd}} \frac{B_t^2}{(B + B_e)^2 + \delta B_e^2}. \quad (6)$$

As already discussed above, this process is responsible for the narrow dip observed in the experiments near zero magnetic field. Besides this term, we also take into account a field-independent term, $1/\tau_{N1}$, to describe the observed millisecond relaxation at moderate external magnetic fields. As a result, the total relaxation rate of the nuclear spin polarization in Eq. (5) is: $1/\tau_N = 1/\tau_{N0} + 1/\tau_{N1}$.

The magnetic-field dependence of the DNP is closely connected to the field dependence of the electron-spin polarization which is calculated by

$$S_z(B) = S_0 [\cos \theta(B)]^2 = S_0 \frac{(B + B_N + B_{fz})^2}{(B + B_N + B_{fz})^2 + B_{fp}^2}, \quad (7)$$

where S_0 is the initial electron-spin polarization created by optical excitation.

To estimate the average value of B_{fp} , we have measured the polarization dip for fast excitation polarization modulation at a frequency of 100 KHz when no DNP field appears. As seen in Fig. 6(b), the dip is centered at zero external magnetic field in this case. Its HWHM gives a measure of the transverse component of the nuclear spin fluctuations: $B_{fp} = 18$ mT.³³

Calculations of the time dependencies of B_N and S_z were done using Eqs. (5) and (7) for different values of the NSF components, $B_{f\alpha}$, $\alpha=x, y$, and z at fixed external magnetic field B . Then the spin polarization S_z was averaged over the fluctuations assuming a Gaussian distribution for their probability density¹⁵

$$w(B_{f\alpha}) = \frac{1}{\sqrt{2\pi}\Delta_\alpha} \exp\left(-\frac{B_{f\alpha}^2}{2\Delta_\alpha^2}\right), \quad (8)$$

where Δ_α is the width of the Gaussian distribution which can be obtained from the experimentally determined fluctuation field by:²³ $\Delta_\alpha = B_{fp}/\sqrt{2}$. The calculations were performed for different values of B to determine the magnetic field dependence of S_z at different times.

Examples of the calculation results are given in Fig. 6(c). Qualitative agreement of the temporal evolution of the dip profile with the one observed in experiments is seen [compare with Fig. 4(b)]. The calculated curves reproduce well the decrease in the dip depth with increasing nuclear field. To obtain the dynamics of the nuclear field from these calculations, we used the same fitting procedure as for the experimental curves as discussed above. The time dependence of the calculated dip position determined in that way shows reasonable agreement with the experimental one, see Fig. 4(c).

For simplification of the calculations, we did not consider a possible spread of the nuclear field arising from variations in P and τ_N in the QD ensemble. We suppose that this spread is responsible for the widening of the polarization dip with excitation density increase as shown in Fig. 3(b). Probably this is the reason why the dip width in the calculated curves is found to be somewhat smaller than in experiment [compare with Fig. 4(c)].

The developed model allows us to extract the dynamics of DNP for different strengths of the external field B . The corresponding results are shown in Fig. 7 as a two-dimensional plot. The dynamics of the polarization dip determined by the condition $B_N = -B$ is also shown there by the thick black line. This dynamics almost exactly coincides with the theoretical curve and, correspondingly, with the experiment data shown in Fig. 4(c). The reasonable agreement with the measurement allows us to conclude that the model reproduces well the temporal evolution of the electron-nuclear spin system for

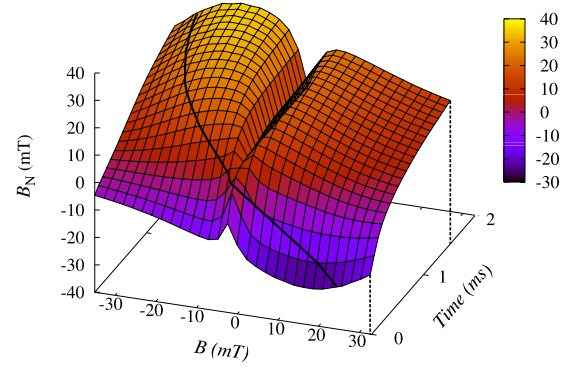


FIG. 7. (Color online) Simulation of time dependence of nuclear field for different external magnetic fields obtained by numerical solution of Eq. (5). Parameters of calculations are the same as for Fig. 6. The thick black line shows intersection of the calculated surface by the plain $B = -B_N$ which indicates the dynamics of polarization dip.

experimental conditions under which the QDs were studied. We want to stress that, though our experimental method gives only partial information about the nuclear field dynamics, the modeling is able to describe the whole DNP dynamics.

In the frame of the considered model, one can easily understand the nonlinear temporal change in the DNP field, shown in Fig. 4(c). At the end of the preceding period of excitation modulation, the DNP field reaches its maximum value. In accordance with Eqs. (3) and (5), the rate of nuclear spin polarization, which determines the slope of the curve in Fig. 4(c), should be minimal at this time. Near the middle of the modulation half period, the DNP field decreases to zero and the rate of nuclear spin polarization increases to its maximum value. Further growth of the DNP field toward the end of the half period reduces the rate of polarization again. Relaxation of the nuclear spin polarization is partially responsible for deceleration of the polarization at the end of the half period and for acceleration of the nuclear spin relaxation at its beginning.

VI. DISCUSSION

Our experimental study, supported by the phenomenological modeling, shows that the nuclear-field rise is considerably slowed down when the nuclear field reaches values exceeding the effective field of the nuclear spin fluctuations which is about 20 mT for the QDs under study.

Two reasons for the saturation of the nuclear field at such a low level for moderate optical pumping exist. First, the pumping rate decreases when the nuclear field becomes large and the electron-spin precession angle θ decreases. Second, the relaxation time of the weak obtained nuclear fields is surprisingly short as already discussed.

The nuclear spin relaxation time is in good accord with the one reported for a single (In,Ga)As/GaAs QD containing a resident electron.⁶ A channel of nuclear-polarization decay should be relaxation via interaction with the resident electron which appears to be quite efficient as compared to direct

diffusion into the surrounding material via dipole-dipole interaction of the nuclear spins. The latter is blocked by the external magnetic field and also by the Knight field of the resident electron. The authors of Ref. 6 demonstrated that by removing the resident electron from the QD the nuclear relaxation time is elongated by three orders of magnitude, from milliseconds to seconds. The authors suggested that the resident electron may lead to indirect coupling of nuclear spins. Our experimental results confirm fast relaxation of the nuclear spin polarization in singly charged QDs.

VII. CONCLUSIONS

We have demonstrated that the technique of optical electron-spin orientation through NCP allows one to study the dynamics of nuclear spin polarization in a QD ensemble. We found that the behavior of the nuclear spin system in singly charged (In,Ga)As/GaAs QDs is highly nontrivial and is determined by the angular momentum transfer from the optically polarized electron spin to the nuclei. We also studied the nuclear spin relaxation after blocking the optical excitation. For moderate excitation densities, the relaxation time is surprisingly short—on the order of milliseconds

rather than seconds, as often assumed. The origin of such a fast relaxation is related to the presence of the resident electron in the QD. Still the underlying mechanisms need to be studied in further detail.

By exploiting the developed experimental method, we managed to study the dynamics of relatively small nuclear fields (tens of milliTesla) created in the QD ensemble by optical pumping with not too high excitation densities. Strong pumping of the electron-nuclei spin system gives rise to a disappearance of the electron-spin polarization dip because the electron-spin depolarization is blocked as well as to a large spread of the nuclear fields so that no reliable information from these experiments can be obtained.

Developing experimental methods to study the regime of strong nuclear fields in QD ensembles is an important task for the near future.

ACKNOWLEDGMENTS

The work was supported by the Russian Foundation for Basic Research, the Ministry of Education and Science of Russian Federation, and the Deutsche Forschungsgemeinschaft (Grant No. BA 1549/12-1). R.V.C. thanks the Government of St.-Petersburg.

-
- ¹*Optical Orientation*, edited by F. Meier and B. P. Zakharchenya (North-Holland, Amsterdam, 1984).
- ²V. K. Kalevich, K. V. Kavokin, and I. A. Merkulov, in *Spin Physics in Semiconductors*, Springer Series in Solid State Science Vol. 157, edited by M. I. Dyakonov (Springer, Berlin, 2008), Chap. 11, p. 309.
- ³D. Gammon, Al. L. Efros, T. A. Kennedy, M. Rosen, D. S. Katzer, D. Park, S. W. Brown, V. L. Korenev, and I. A. Merkulov, *Phys. Rev. Lett.* **86**, 5176 (2001).
- ⁴R. Oulton, A. Greulich, S. Yu. Verbin, R. V. Cherbunin, T. Auer, D. R. Yakovlev, M. Bayer, I. A. Merkulov, V. Stavarache, D. Reuter, and A. D. Wieck, *Phys. Rev. Lett.* **98**, 107401 (2007).
- ⁵A. I. Tartakovskii, T. Wright, A. Russell, V. I. Fal'ko, A. B. Van'kov, J. Skiba-Szymanska, I. Drouzas, R. S. Kolodka, M. S. Skolnick, P. W. Fry, A. Tahraoui, H.-Y. Liu, and M. Hopkinson, *Phys. Rev. Lett.* **98**, 026806 (2007).
- ⁶P. Maletinsky, A. Badolato, and A. Imamoglu, *Phys. Rev. Lett.* **99**, 056804 (2007).
- ⁷B. Pal, S. Yu. Verbin, I. V. Ignatiev, M. Ikezawa, and Y. Masumoto, *Phys. Rev. B* **75**, 125322 (2007).
- ⁸B. Urbaszek, P.-F. Braun, T. Amand, O. Krebs, T. Belhadj, A. Lemaître, P. Voisin, and X. Marie, *Phys. Rev. B* **76**, 201301(R) (2007).
- ⁹A. V. Khaetskii, D. Loss, and L. Glazman, *Phys. Rev. Lett.* **88**, 186802 (2002).
- ¹⁰A. Imamoglu, E. Knill, L. Tian, and P. Zoller, *Phys. Rev. Lett.* **91**, 017402 (2003).
- ¹¹L. M. Woods, T. L. Reinecke, and A. K. Rajagopa, *Phys. Rev. B* **77**, 073313 (2008).
- ¹²W. A. Coish and D. Loss, *Phys. Rev. B* **70**, 195340 (2004).
- ¹³H. Christ, J. I. Cirac, and G. Giedke, *Phys. Rev. B* **75**, 155324 (2007).
- ¹⁴G. G. Kozlov, *Zh. Eksp. Teor. Fiz.* **132**, 918 (2007) [*JETP* **105**, 803 (2007)].
- ¹⁵I. A. Merkulov, Al. L. Efros, and M. Rosen, *Phys. Rev. B* **65**, 205309 (2002).
- ¹⁶A. Greulich, R. Oulton, E. A. Zhukov, I. A. Yugova, D. R. Yakovlev, M. Bayer, A. Shabaev, Al. L. Efros, I. A. Merkulov, V. Stavarache, D. Reuter, and A. Wieck, *Phys. Rev. Lett.* **96**, 227401 (2006).
- ¹⁷R. I. Dzhoiev, B. P. Zakharchenya, V. L. Korenev, P. E. Pak, D. A. Vinokurov, O. V. Kovalenkov, and I. S. Tarasov, *Fiz. Tverd. Tela* **40**, 1745 (1998) [*Phys. Solid State* **40**, 1587 (1998)].
- ¹⁸S. Cortez, O. Krebs, S. Laurent, M. Senes, X. Marie, P. Voisin, R. Ferreira, G. Bastard, J.-M. Gérard, and T. Amand, *Phys. Rev. Lett.* **89**, 207401 (2002).
- ¹⁹M. Ikezawa, B. Pal, Y. Masumoto, I. V. Ignatiev, S. Yu. Verbin, and I. Ya. Gerlovin, *Phys. Rev. B* **72**, 153302 (2005).
- ²⁰M. E. Ware, E. A. Stinaff, D. Gammon, M. F. Doty, A. S. Bracker, D. Gershoni, V. L. Korenev, S. C. Badescu, Y. Lyanda-Geller, and T. L. Reinecke, *Phys. Rev. Lett.* **95**, 177403 (2005).
- ²¹A. Shabaev, E. A. Stinaff, A. S. Bracker, D. Gammon, A. L. Efros, V. L. Korenev, and I. Merkulov, *Phys. Rev. B* **79**, 035322 (2009).
- ²²I. V. Ignatiev, S. Yu. Verbin, I. Ya. Gerlovin, R. V. Cherbunin, and Y. Masumoto, *Opt. Spectrosc.* **106**, 375 (2009).
- ²³M. Yu. Petrov, I. V. Ignatiev, S. V. Poltavtsev, A. Greulich, A. Bauschulte, D. R. Yakovlev, and M. Bayer, *Phys. Rev. B* **78**, 045315 (2008).
- ²⁴C. W. Lai, P. Maletinsky, A. Badolato, and A. Imamoglu, *Phys. Rev. Lett.* **96**, 167403 (2006).
- ²⁵As seen from Fig. 3(a) the PL polarization changes its sign, i.e.,

- becomes *positive*, at small B when the optical excitation is weak. The origin of this positive polarization can be understood from an analysis of the PL kinetics. The PL polarization is positive right after the excitation (Ref. 18) and then approaches a negative value whose magnitude is small at weak excitation when the relaxation of the electron-spin polarization becomes competitive with the excitation.
- ²⁶M. N. Makhonin, A. I. Tartakovskii, A. B. Van'kov, I. Drouzas, T. Wright, J. Skiba-Szymanska, A. Russell, V. I. Fal'ko, M. S. Skolnick, H.-Y. Liu, and M. Hopkinson, *Phys. Rev. B* **77**, 125307 (2008).
- ²⁷M. I. Dyakonov and V. I. Perel, *Zh. Eksp. Teor. Fiz.* **65**, 362 (1973) [*Sov. Phys. JETP* **38**, 177 (1974)].
- ²⁸B. Eble, O. Krebs, A. Lemaître, K. Kowalik, A. Kudelski, P. Voisin, B. Urbaszek, X. Marie, and T. Amand, *Phys. Rev. B* **74**, 081306(R) (2006).
- ²⁹P. Maletinsky, C. W. Lai, A. Badolato, and A. Imamoglu, *Phys. Rev. B* **75**, 035409 (2007).
- ³⁰T. Belhadj, T. Kuroda, C.-M. Simon, T. Amand, T. Mano, K. Sakoda, N. Koguchi, X. Marie, and B. Urbaszek, *Phys. Rev. B* **78**, 205325 (2008).
- ³¹Absorption of the photon results in creation of an electron-hole pair which relaxes in energy and is coupled with the resident electron in a trion. During this process the wave function and the energy of the resident electron is considerably changed. We assume that it is the process, which allows one to overcome the problem of the energy conservation in the process of transfer of angular momentum from electron to nuclear spins.
- ³²A. Abraham, *Principle of Nuclear Magnetism* (Clarendon, Oxford, 1961), Chap. 2.
- ³³Experimentally, the HWHM of the polarization dip depends on the excitation conditions, in particular, on the excitation density and the laser excitation mode (pulsed or continuous wave). For determining B_{fp} in this work we used the same conditions as for studying the DNP field.